

Article

# Modeling of the Thermal Efficiency of a Whole Cement Clinker Calcination System and Its Application on a 5000 MT/D Production Line

Yanfei Yao <sup>1</sup>, Songxiong Ding <sup>2</sup> and Yanxin Chen <sup>1,\*</sup>

<sup>1</sup> College of Materials Science and Engineering, Xi'an University of Architecture and Technology, Xi'an 710055, China; yyanfxauat@163.com

<sup>2</sup> Department of Civil Engineering, University of Agder, 4879 Grimstad, Norway; songxiong.ding@uia.no

\* Correspondence: chenyanxin@xauat.edu.cn; Tel.: +86-1309-697-3109

Received: 21 August 2020; Accepted: 5 October 2020; Published: 10 October 2020



**Abstract:** This paper proposes that the scope of research should be extended to the whole clinker calcination system from its single device or specific process (i.e., its functional subunits) as conventionally conducted. Mass/heat flow and effective heat were first analyzed to obtain the thermal efficiencies of its subunits ( $\varphi^i$ ); a thermal efficiency model of the whole system  $\varphi^{QY}$  was thus established by correlating the relationship between  $\varphi^i$  and  $\varphi^{QY}$ . The thermal efficiency model of the whole system showed that  $\varphi^i$  had a positive linear correlation with  $\varphi^{QY}$ ; it was found that the thermal efficiency of the decomposition and clinker calcination unit ( $\varphi^{DC}$ ) had the greatest weight on  $\varphi^{QY}$ , where a 1% increase in  $\varphi^{DC}$  led to a 1.73% increase in  $\varphi^{QY}$ —improving  $\varphi^{DC}$  was shown to be the most effective way to improve  $\varphi^{QY}$ . In this paper, the developed thermal efficiency model was applied to one 5000 MT/D production line. It was found that its  $\varphi^{QY}$  was only 61.70%—about 2.35% lower than a representative line; such decrease was caused by its low  $\varphi^{DC}$  and  $\varphi^P$  which, as disclosed by model, were derived from the low decomposition rate of calcium carbonate in preheated meal put into a calciner and the high excess air coefficient of secondary air. Controlled parameter optimization of this 5000 MT/D production line was then carried out. As a result, the  $\varphi^{DC}$  and  $\varphi^P$  of the production line were increased from 30.03% and 64.61% to 30.69% and 65.69%, respectively; the  $\varphi^{QY}$  increased from 61.70% to 62.55%; the clinker output of the production line increased from 5799 MT/D to 5968 MT/D; the heat consumption of clinker was reduced from 3286.98 kJ/kg-cl to 3252.41 kJ/kg-cl.

**Keywords:** thermal efficiency; effective heat; whole system; decomposition rate

## 1. Introduction

Cement clinker manufacturing is an energy-intensive process, often involving fuel (pulverized coal, oil and gas) combustion/firing. Fuel firing (mainly pulverized coal in China) is required to achieve and maintain thermal conditions for carbonate decomposition and clinker calcination; it is also a process with significant CO<sub>2</sub> emissions [1,2]. Global process emissions during cement production in 2017 were 1.48 ± 0.20 GT of CO<sub>2</sub>, equivalent to about four percent of the total global fossil fuel emissions [3]. With the development of suspension preheaters and pre-calciner technology, the capacity of single-cement production lines has been greatly increased at a much-reduced energy consumption rate [4,5]. The maximum production scale of a cement production line can reach 12,000 MT/D at a heat consumption of as low as 2900 kJ/kg-cl [6]. Benefiting from continuous technological advances, the modern cement industry has become more conscious of the energy efficiency of the whole production line while pursuing increased capacities of cement kilns.

It is estimated that 95% of the energy consumption in cement clinker production comes from thermal energy; fuel consumption accounts for 50–60% of the total costs of cement production [7].

Therefore, there are economic reasons to improve the energy efficiency of production lines. In fact, considerable efforts have been made to improve the performance of various thermal devices as adopted in cement clinker production to reduce fuel consumption [8,9]. Typical examples include implementation of large scale NSP (New Suspension Preheater) kilns and high-performance burners, the development of advanced raw meal preheaters and calciner units based on “high solid-gas ratio technology” and other efforts to develop production lines with external processing of coal grinding and raw meal drying to retrieve the thermal energy exiting the flues [10–13]. It is worth noting that research has been recently conducted to develop intelligent control tools for the same purpose [14–18].

For cement clinker calcination systems, improving thermal efficiency is the most direct way to reduce heat consumption [19], and the key to increasing heat efficiency lies in how to determine the key parameters and their most valuable operating range. The modern cement industry mostly uses distributed control systems to control operating parameters [20]. Assuming a 2500 MT/D cement production line as an example, there are more than 2000 operating parameters, and most of the parameters affect and restrict each other, which means that it is quite challenging to improve thermal efficiency in a simple fashion [21,22].

Rasul M. G. adopted burning and second law efficiencies and cooler and recovery efficiencies to assess the thermal performance of the cement industry in Indonesia [8]. In doing so, thermal energy conservation opportunities were also identified. Liu Z. established a thermally efficient analytical model of raw material preheating and decomposition, clinker calcination and clinker cooling and determined that increasing the raw material decomposition rate fed into the kiln can improve the thermal efficiency of the clinker calcination process unit [23]. It should be noted that research on thermal efficiency is mostly concentrated on a single device or unit, and studies encompassing the whole cement production system have not been sufficiently carried out.

This paper proposes that the scope of research should be extended from a single device or certain process to the whole cement clinker calcination system (the whole system) while analyzing the thermal efficiency of the cement clinker production process. The whole system has been divided into five subunits based on the production process, and the subunits have been further divided into heat firing units and heat recovery units, according to the functions of the main thermal equipment in their respective scope. Thus, the effective heat and thermal efficiency of the whole system and its five subunits have been identified using mass and energy balances, and the relationships between the thermal efficiencies of the subunits and thermal efficiency of the whole cement clinker system have been analyzed to establish the thermal efficiency model of the whole system. This thermal efficiency model has also been applied to a 5000 MT/D production line.

## 2. Scope and Objectives of the Whole System

Taking one 5000 MT/D cement clinker production line in Anhui Province as an example, a modern cement production line typically consists of eight thermal devices: the raw mill, SP waste heat boiler, preheater, calciner, rotary kiln, grate cooler, coal mill, and AQC waste heat boiler. Based on energy/mass flows and the functionality of each device, they have been grouped into five subunits (as illustrated in Figure 1):

- a. Raw Material Grinding and Boiler of Suspension Preheater (SP) unit (R&SP) for handling raw material and cogeneration.
- b. Preheating unit as row feed preheaters.
- c. Decomposition and Clinker Calcination unit (D&C) for the formation of clinker.
- d. Clink Cooling unit (grate cooler) for the rapid cooling of hot clinker.
- e. Coal Grinding and Boiler of Air Quenching Cooler (AQC) unit (C&AQC) for handling raw coal and cogeneration.

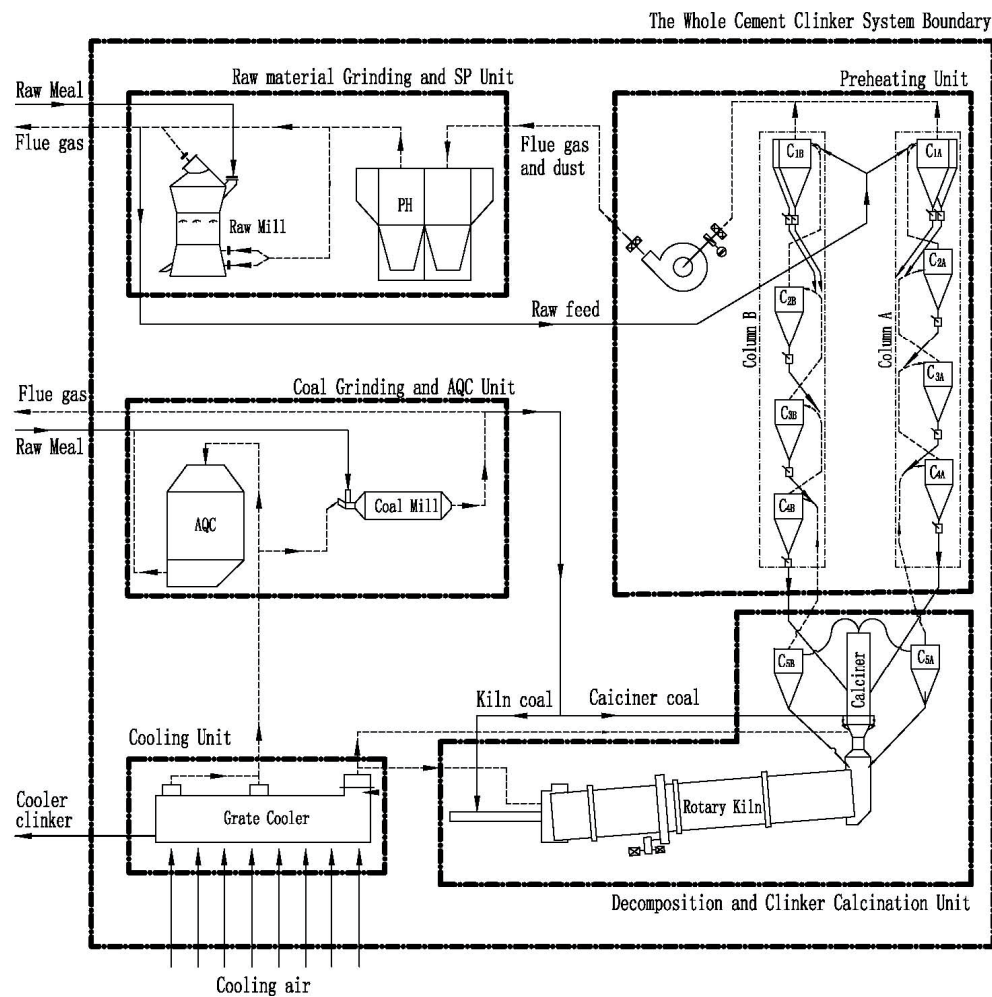


Figure 1. Whole system and its subunits in a modern cement production line.

Figure 1 shows the mass flow between the various units either as inputs or as outflow/output to be defined and clarified later for the whole system. The raw mill is used to dry and grind wet raw materials to a required particle size as raw feed, and the raw feed is then fed into the Preheating unit for heating. Such raw feed is expected to be heated to 750–790 °C from ambient temperature before entering the D&C unit. As shown in Figure 1, pulverized coal is burned in the calciner for decarbonation of the heated raw feed and the rotary kiln for the formation reaction of the clinker, respectively. The newly formed clinker exits to the Cooling unit for rapid cooling. The Cooling unit (grate cooler) utilizes air to quench the clinker, and as a result, the air itself can be quickly heated. The air is then sent into different pieces of equipment: air at medium and low temperatures is sent to the C&AQC unit for drying raw coal and power generation, while air at high temperature is sent to the D&C unit as “secondary air” or “tertiary air” to provide oxygen for the combustion of pulverized coal in the rotary kiln or calciner. All air is now becoming ‘flue gas’, which is then introduced to the R&SP unit after heat exchange with raw materials in the Preheating unit.

### 3. Effective Heat and Thermal Efficiency

#### 3.1. Definition of Effective Heat and Thermal Efficiency

Heat balance analysis was introduced to address both the input and output heats of the whole system and its subunits, and the output heat was further divided into three categories according to consumption method, which are effective heat, transfer heat and lost heat. Among them, effective

heat refers to the heat directly consumed to realize the purpose of the subunits or the whole system, transfer heat refers to the heat that cannot be fully used by one subunit and is transferred to adjacent subunits in the form of sensible heat carried by flue gas and materials, lost heat refers to the heat lost during the utilization and transmission of heat, mostly in the form of surface heat loss, sensible heat contained in the low temperature flue gas and materials discharged from the whole system.

The purposes of the subunits and whole system are determined by their main thermal devices, which can be categorized as calcination devices and heat recovery devices. For the whole kiln system, only the decomposition calciner (D&C unit) and rotary kiln belong to calcination devices, while all other thermal equipment belongs to heat recovery devices. Therefore, the D&C unit is the only calcination unit of all subunits within which pulverized coal is burned to provide the necessary heat to form cement clinker [19]; its effective heat refers to the heat consumed by the physical and chemical reactions during clinker generation, such as decomposition heat of calcium carbonate and the formation heat of clinker. Heat recovery units, including the R&SP unit, Preheating unit, Cooling unit, and C&AQC unit, can recover heat from the high temperature flue gas and hot-red clinker to be used in various ways, such as drying materials, residual heat power generation and preheating raw materials. For one specific subunit, its effective thermal reference would be analyzed in the following specific articles/sections.

The ratio of effective heat to the sum of the input heat is defined as the thermal efficiency of the subunit or whole system:

$$\varphi_i = \frac{E_U^i}{E_{in}^i}. \quad (1)$$

where  $\varphi_i$  is the thermal efficiency of the whole system or its subunit (%), where a larger thermal efficiency value relates to higher heat utilization efficiency of the subunit or the whole system.  $E_u$  is the effective heat (kJ) and  $E_{in}$  is the total input heat (kJ). The symbol "i" in Equation (1) refers to different objectives, RS for R&SP unit, P for Preheating unit, DC for D&C unit, C for Cooling unit, CA for C&AQC unit and QY for the whole system. For instance,  $\varphi_{RS}$  is the energy efficiency of the R&SP unit, and  $E_U^{CA}$  is the effective heat utilized by the C&AQC unit.

### 3.2. Assumptions

Calculation and analysis of all heat measurements in this paper were calculated by thermodynamic principles with assumptions as follows.

1. The whole cement clinker system is stable, i.e., in a steady state.
2. All calculations are based on one kilogram of clinker.
3. Ambient temperature (20 °C) was used as the reference temperature; therefore, sensible heat of normal temperature materials and air entering the system, such as raw materials, coal and cooling air, can be ignored.
4. No air seepage occurred in the whole system.

### 3.3. Effective Heat of Subunits

#### 3.3.1. Raw Material Grinding and SP Unit (R&SP)

The Raw Material Grinding and SP unit has two main devices: the SP waste heat boiler and the raw mill, as shown in Figure 2.

Sensible heat of the flue gas (denoted as  $Q_{YQ}$ ) from the Preheating unit and the sensible heat of fly ash contained in the flue gas ( $Q_{FC}$ ) constitute the input heat of the R&SP unit ( $E_{in}^{RS}$ ). That is:

$$E_{in}^{RS} = Q_{YQ} + Q_{FC} \quad (2)$$

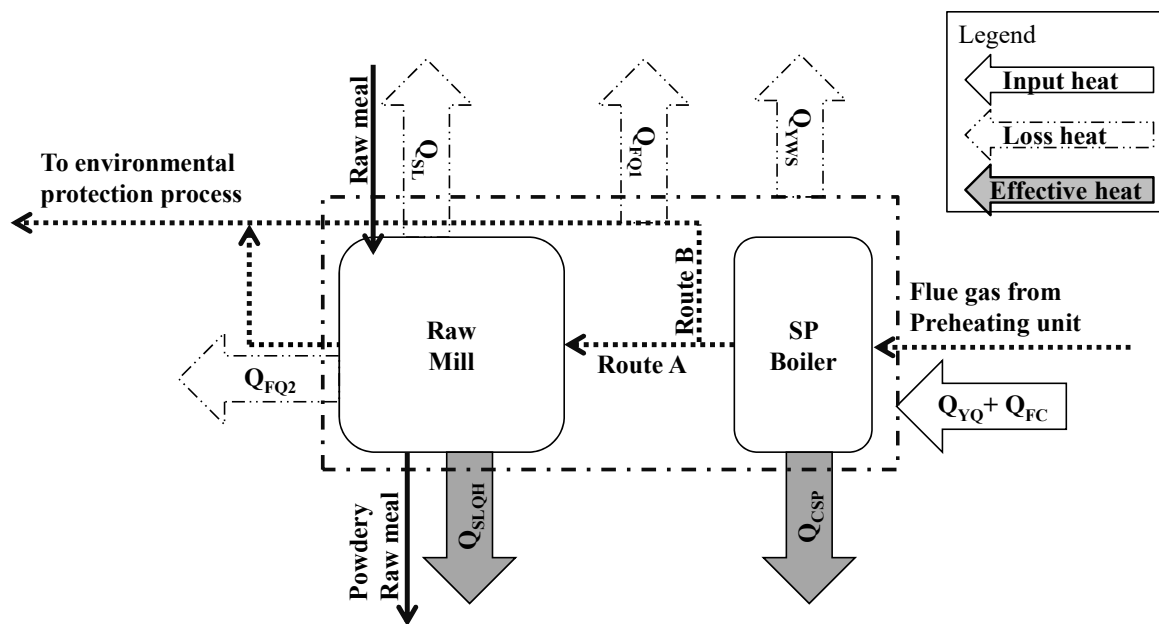


Figure 2. Heat flow modeling of the Raw Material Grinding and SP unit.

Flue gas from the Preheating unit with a temperature of 270~340 °C first goes through the SP boiler to heat circulating water in the SP boiler to obtain superheated steam; the heat obtained by the circulating water constitutes the first effective heat of the R&SP unit, which is denoted as  $Q_{CSP}$ . Flue gas discharged from the SP boiler is then divided into two routes, 90% of which enters the raw mill (route A in Figure 2) to dry the wet raw material while the other 10% (route B in Figure 2) enters the process with the flue gas and powdered dry raw mill discharged from the raw mill for further environmental protection treatment, where the powdered raw mill can be collected. Heat consumed to evaporate the moisture in the raw material constitutes the second effective heat of the R&SP unit and is denoted as  $Q_{SLQH}$ ; thus, the effective heat  $E_U^{RS}$  of the R&SP unit can be calculated by Equation (3):

$$E_U^{RS} = Q_{CSP} + Q_{SLQH} \quad (3)$$

Sensible heat of both the exhaust gas and powdered dry raw mill at the R&SP outlet cannot be used by any other equipment or subunit and is considered as heat loss together with the heat dissipation through the R&SP surface.

Heat flows of the Raw Material Grinding and SP unit are shown in Figure 2 and its heat balance is given in Table 1 with brief descriptions. All heat involved in this article can be classified into three types: chemical reaction, sensible heat and surface heat loss; their calculated values are shown in Table 1. For conciseness in the subsequent analysis, only the calculation of chemical heat is specified, whereas the calculation processes of surface heat dissipation and physical heat will not be described.

**Table 1.** Heat balance of the Raw Material Grinding and SP (R&SP) unit.

Input Heat		
Symbols	Description	Formula Used
$Q_{YQ}$	Sensible heat of flue gas at preheater outlet	$A_1 \cdot C_1 \cdot (T_1 - T_0)$
$Q_{FC}$	Sensible heat of fly ash at preheater outlet	$M_1 \cdot C_2 \cdot (T_2 - T_0)$
$E_{in}^{RS}$	Total input heat of R&SP unit	$\Sigma Q_i$
Output heat		
Item Symbols	Description	Formula used
Lost heat $Q_{FQ}$	Sensible heat of exhaust gas at R&SP outlet	$A_2 \cdot C_3 \cdot (T_3 - T_0)$
Lost heat $Q_S$	Heat dissipation of R&SP surface	$\xi_1 \cdot S_1 \cdot (T_5 - T_0)$
Lost heat $Q_{SL}$	Sensible heat of raw materials at raw mill outlet	$M_2 \cdot C_4 \cdot (T_4 - T_0)$
Effective heat $Q_{SLQH}$	Heat consumption of water evaporation	$M_3 \cdot 2496$
Effective heat $Q_{CSP}$	Absorbed heat by SP boiler	$M_4 \cdot (C_6 \cdot T_7 - C_5 \cdot T_6)$
$E_{out}^{RS}$	Total output heat of R&SP unit	$\Sigma Q_i$

### 3.3.2. Preheating Unit

The Preheating unit contains 10 cyclones which are arranged on four levels in twin-parallel columns, A and B; in each column, there are two cyclones on level one and one cyclone from levels two to four downward, which are named as  $C_{1A1/A2}$ ,  $C_{2A}$ ,  $C_{3A}$ ,  $C_{4A}$ ,  $C_{1B1/B2}$ ,  $C_{2B}$ ,  $C_{3B}$  and  $C_{4B}$  for convenience (see Preheating unit in Figure 1). The hot flue gas exiting from the D&C unit is streamed evenly into columns A and B through each upward cyclone, and the raw feed is fed into cyclones  $C_{1A1/A2}$  and  $C_{1B1/B2}$ , respectively.

The purpose of the preheating system is to recover the heat in the high temperature flue gas and fly ash from the D&C unit to heat the fed raw feed. All of its input heat comes from the sensible heat of hot air and fly ash from the D&C unit (denoted as  $Q_{C5F}$ ).

Chemical reactions, such as the decomposition of magnesium carbonate, occur during the preheating process; the heat required in such a process is called the formation heat of clinker in the Preheating unit (denoted as  $Q_{SC1}$ ) and belongs to effective heat. The formula of  $Q_{SC1}$  is as follows:

$$Q_{SC1} = M_5 \cdot 1420 \quad (4)$$

The effective heat of the Preheating unit ( $E_U^P$ ) refers to the sum of the heat absorbed by the preheated raw feed (denoted as  $Q_{C4}$ ) and the formation heat of clinker in the Preheating unit (see Equation (5)).

$$E_U^P = Q_{SC1} + Q_{C4} \quad (5)$$

Flue gas, after heat exchange with the raw feed, as well as a small amount of dust carried in the flue gas, is discharged from  $C_{1A1/A2}$  and  $C_{1B1/B2}$  and enters the SP boiler in the R&SP unit, where the sensible heat can be recycled. Then, the sensible heat of the flue gas and fly ash at the preheater (denoted as  $Q_{YQ}$  and  $Q_{FC}$ ) outlet can be classified as transfer heat. The only lost heat in the Preheating unit is the heat dissipation of the Preheating unit surface (denote as  $Q_{YRS}$ ). Heat flow modeling of the Preheating unit is shown in Figure 3.

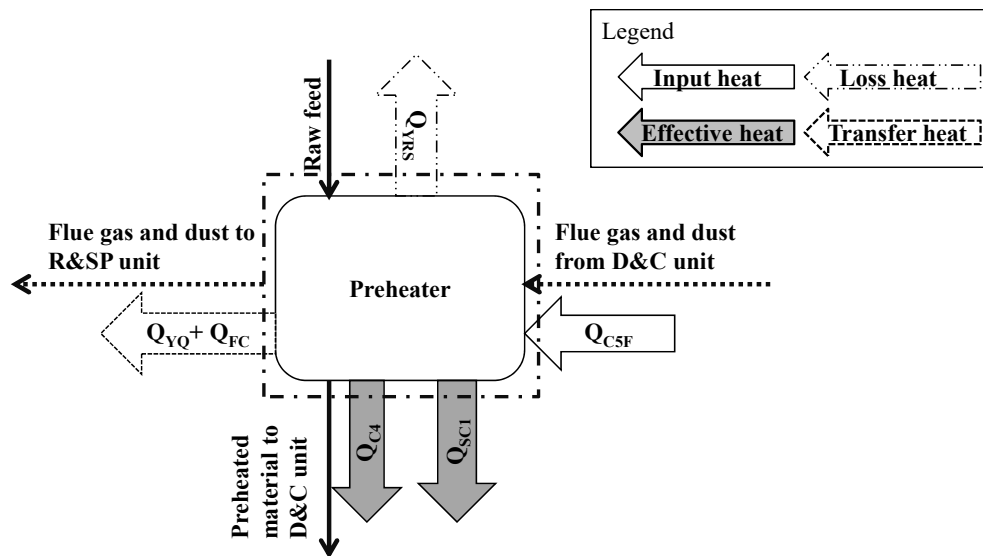


Figure 3. Heat flow modelling of the Preheating unit.

### 3.3.3. Decomposition and Clinker Calcination Unit (D&C unit)

The Decomposition and Clinker Calcination unit (D&C subunit) consists of the calciner, cyclone  $C_{5A/B}$ , tertiary air ducts and a rotary kiln. Most cement enterprises use pulverized coal as fuel, 30–40% of which ( $M_{TM}$  in Figure 1) is fed into the rotary kiln and the other 60–70% ( $M_{WM}$  in Figure 1) into the calciner; under the action of heat and oxygen provided by high temperature air from the Cooling unit, pulverized coal burns and releases heat, which can be denoted as  $Q_{TM}$  and  $Q_{WM}$ , respectively. Exothermic combustion of pulverized coal, as well as the sensible heat of high temperature tertiary air and secondary air from the Cooling unit (denoted as  $Q_{3C}$  and  $Q_{2C}$ , respectively) and heated material/feed from the Preheating unit (denoted as  $Q_{C4}$ ), are composed of the input heat in the D&C subunit.

As the only calcination unit in the whole system, the purpose of the D&C unit is to provide a high temperature environment and steady stream of heat required to carry out the chemical reaction to form the clinker. Chemical reactions in the D&C unit can be divided into two categories: decomposition of calcium carbonate and formation of clinker; the heat consumed in these reactions is countered as the effective heat of the D&C unit and can be calculated by formulas (6–8).  $C_3S$ ,  $C_2S$ ,  $C_3A$  and  $C_4AF$  in Equation (8) are the percentages of various minerals in clinker, which can be concluded from the composition analysis of clinker.

$$E_U^{DC} = Q_{SC2} + Q_{SC3}. \quad (6)$$

$$Q_{SC2} = M_6 * 1686 \quad (7)$$

$$Q_{SC3} = -(C_3S*465 + C_2S*610 + C_3A*88 + C_4AF*105)/100 \quad (8)$$

After the completion of the reactions in the D&C subunit, spherical clinker is formed and transported to the Cooling unit at a temperature of about 1400 °C for rapid cooling, whereas the 870 °C flue gas is discharged from the cyclone  $C_5$  outlet and streamed into the Preheating unit. Sensible heat of the flue gas and dust (denoted as  $Q_{C5F}$ ) can be reused as the heat source for preheating raw meal, and the sensible heat of red-hot clinker (denoted as  $Q_{HS}$ ) can also be recycled in the Cooling unit, both of which are classified as transfer heat of the D&C unit.

The only heat loss of the D&C unit is the dissipated heat through the calciner surface, cyclone  $C_{5A/B}$ , tertiary air duct and rotary kiln (denoted as  $Q_{DCS}$ ). It is worth noting that  $Q_{DCS}$  is usually considerable, greater than that of all other subunits because of the high surface temperature of the D&C unit (the surface temperature of the rotary kiln is much higher than that of all other thermal equipment in the whole system).

The heat flow of the D&C unit is shown in Figure 4.

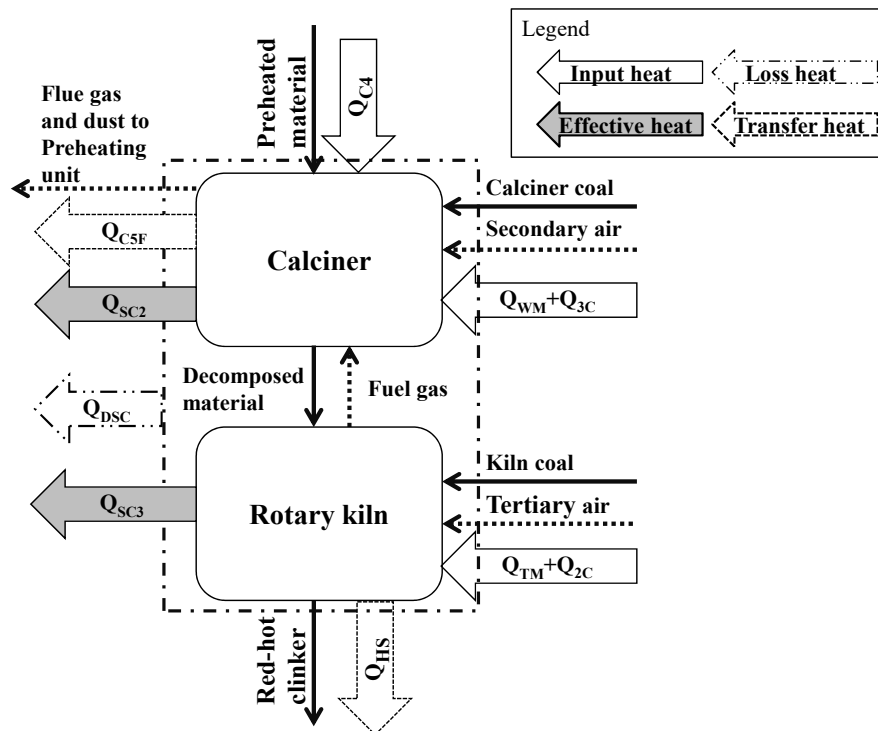


Figure 4. Heat flow modelling of the Decomposition and Clinker Calcination unit.

### 3.3.4. Cooling Unit

Red-hot clinker discharged from the rotary kiln moves along the grate bed of the grade cooler to complete rapid heat exchange with ambient temperature cooling air, where the temperature of discharged clinker from the grade cooler can be reduced from about 1400 °C to about 100 °C and the cooling air temperature conversely increases. As the most important heat recovery device in the whole system, the Cooling unit plays an important role in reducing the heat consumption of clinker burning.

The input heat of the Cooling unit ( $E_{in}^C$ ) is the sensible heat of red-hot clinker (denoted as  $Q_{HS}$ ), most of which is utilized as the sensible heat of hot cooling air after heat exchange. Cooling air discharged from the front of the grate bed has a high temperature and is sent to the D&C subunit as “secondary air” and “tertiary air” to provide oxygen and heat for coal combustion; their heat is denoted as  $Q_{2C}$  and  $Q_{3C}$ , respectively. Cooling air discharged from the middle and back section of the grate bed is generally used for waste heat power generation and drying raw coal for its low temperature; its heat is denoted as  $Q_{ZWF}$ .

The effective heat of the Cooling unit ( $E_U^C$ ) refers to the sum of the sensible heat of all hot cooling air, which is calculated as follows:

$$E_U^C = Q_{3C} + Q_{2C} + Q_{ZWF} \quad (9)$$

Lost heat of the Cooling unit contains both the dissipated heat through its surface (denoted as  $Q_{LQS}$ ) and the sensible heat of cooled clinker at the grate cooler outlet (denoted as  $Q_{CS}$ ). The heat flow of the Cooling unit is shown in Figure 5.

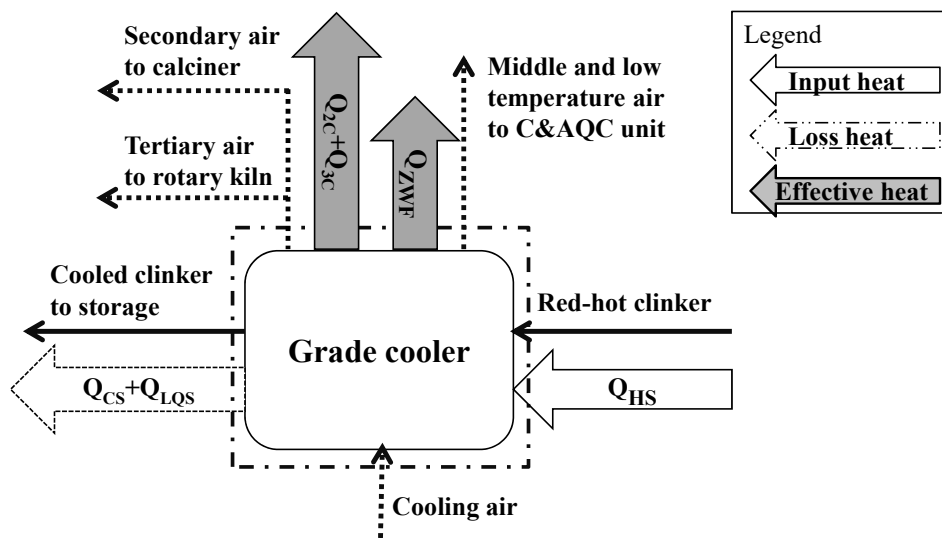


Figure 5. Heat flow modelling of the Cooling unit.

### 3.3.5. Coal Grinding and AQC Unit

The C&AQC unit has a similar process and function as the R&SP unit, but the difference is that the C&AQC unit uses the middle and low temperature air from the Cooling unit ( $Q_{ZWF}$ ) as the input heat. The heat balance of the C&AQC unit is given in Table 2, where heat input, effective heat and lost heat (Heat outflow) have been identified.

Table 2. Heat balance of the C&AQC unit.

Heat Input		
Symbols	Description	
$Q_{ZWF}$	Sensible heat of middle and low temperature air	
$E_{in}^{CA}$	Total heat input of C&AQC unit	
Heat Out		
Symbols	Description	
Lost heat	$Q_{YTF}$	Sensible heat of exhaust gas at the C&AQC outlet
Lost heat	$Q_{YTS}$	Heat dissipation of the C&AQC surface
Lost heat	$Q_{MF}$	Sensible heat of coal at coal mil outlet
Effective heat	$Q_{AQC}$	Absorbed heat by AQC boiler
Effective heat	$Q_{MFQH}$	Heat consumption of water evaporation in coal
$E_{out}^{CA}$	Total heat output of C&AQC unit	

### 3.3.6. Effective Heat of the Whole System

The purpose of the whole system can be divided into two categories: one is to provide the heat needed for clinker generation and the other is to recover the heat in the discharged flue gas during the burning process.

The input heat of the whole system  $E_{in}^{QY}$  is the combustion heat from pulverized coal where ambient temperature is used as the reference temperature, and most is used to form clinker. The formation heat of clinker is denoted as  $Q_{SC}$ , which is the sum of  $Q_{SC1}$ ,  $Q_{SC2}$ , and  $Q_{SC3}$ . About 30% of  $E_{in}^{QY}$  is consumed in the form of sensible heat of medium and low temperature flue gas at the outlets of both the Preheating and Cooling units, which can be reused for drying raw coal and materials and power generation. Lost heat of the whole system includes surface heat loss during heat utilization and recovery, and the sensible heat of the exhaust gas and cooled clinker discharged from the R&SP and C&AQC units. There is no transfer heat when taking the whole system as the research object.

The heat flow of the whole system is shown in Figure 6.

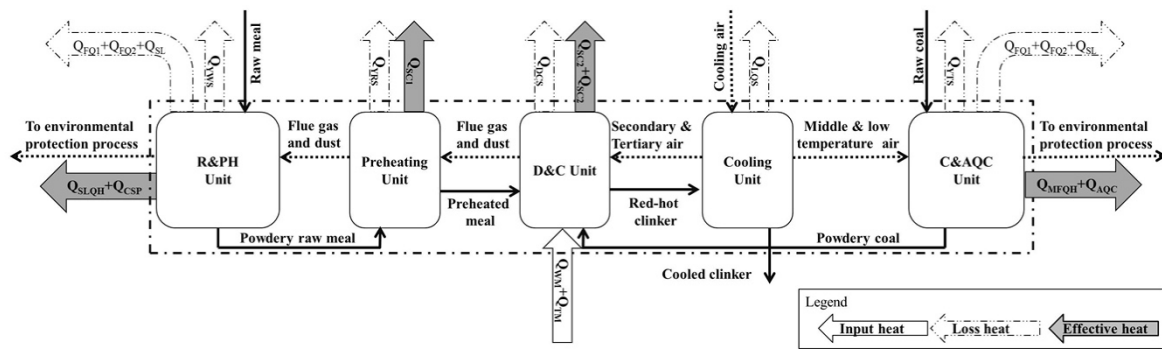


Figure 6. Heat flow modeling of the whole system.

#### 4. Modeling of the Thermal Efficiency of the Whole Cement Clinker System

As defined in Section 3.3, the thermal efficiency of the whole system could be written as:

$$\varphi^{QY} = \frac{E_U^{QY}}{E_{in}^{QY}} \tag{10}$$

By introducing the thermal efficiency of each subunit, the thermal efficiency of the whole system  $\varphi^{QY}$ , as expressed in Equation (10), can be modified as follows:

$$\varphi^{QY} = 1 - \frac{E_{in}^{CA}}{E_{in}^{QY}} - \frac{E_{in}^{DC}}{E_{in}^{QY}} + \varphi^{CA} \frac{E_{in}^{CA}}{E_{in}^{QY}} + \varphi^P \frac{E_{in}^P}{E_{in}^{QY}} + \varphi^{DC} \frac{E_{in}^{DC}}{E_{in}^{QY}} + \varphi^C \frac{E_{in}^C}{E_{in}^{QY}} + \varphi^{RS} \frac{E_{in}^{RS}}{E_{in}^{QY}}. \tag{11}$$

where  $\varphi^{RS}$ ,  $\varphi^P$ ,  $\varphi^{DC}$ ,  $\varphi^C$  and  $\varphi^{CA}$  refer to the energy efficiencies for the Raw Material Grinding and SP unit, Preheating unit, Decomposition and Clinker Calcination unit, Cooling unit and Coal Grinding and AQC unit, respectively.

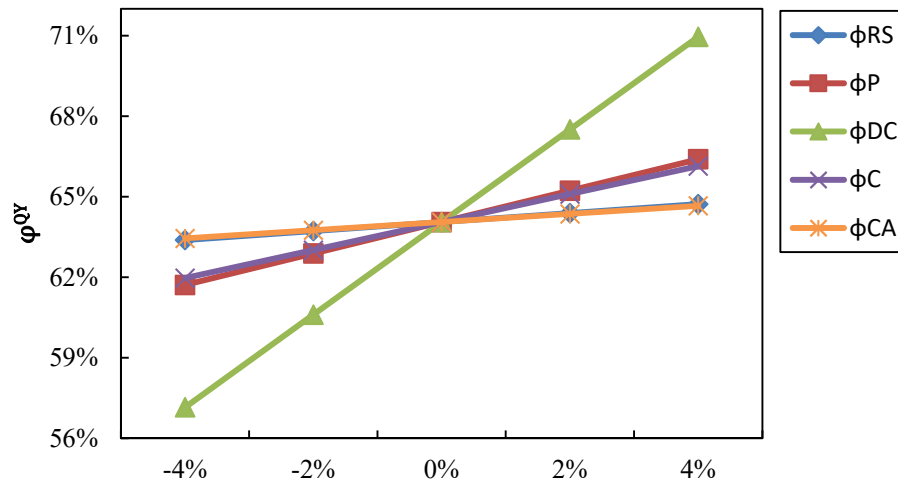
The thermal efficiency model given in (11) shows that  $\varphi^{QY}$  has a positive linear correlation with the thermal efficiencies of all five subunits, meaning that an increase in the thermal efficiency of any subunit will lead to an increase in  $\varphi^{QY}$ .

In industrial production, the thermal efficiencies of subunits affect and restrict each other. For example, a reduction in  $\varphi^C$  will reduce the air temperature entering the D&C and C&AQC units and affect the combustion of both calciner coal and kiln coal, and the heat exchange effect of the coal mill and AQC boiler,  $\varphi^{DC}$  and  $\varphi^{CA}$ , will be reduced. A poor combustion of pulverized coal will reduce the quality and output of clinker, which will further reduce the heat brought into the Cooling unit by hot-red clinker and the heat exchange effect between cooling air and clinker and cause further reductions in  $\varphi^P$ .

Thermal efficiencies of all subunits on one representative 5000 MT/D production line were obtained as reference values of  $\varphi^i$  (as shown in Table 3). To quantitatively analyze the influence of the individual thermal efficiencies of each subunit on the whole system  $\varphi^{QY}$ , the mutual influence of the thermal efficiency between subunits must be controlled—it is hereby assumed that the change in thermal efficiency of one subunit will not affect the thermal efficiency of another subunit. On this basis, the thermal efficiency of one subunit  $\varphi^i$  was maneuvered with an increase or decrease by an increment of 2%, and the contribution of such changes to the thermal efficiency of the whole system  $\varphi^{QY}$  was calculated according to the thermal efficiency model as given in (11); the result is shown in Figure 7.

**Table 3.** Thermal efficiencies of subunits of a representative 5000 MT/D production line.

Item	Units	R&S Unit	Preheating Unit	D&C Unit	Cooling Unit	C&A Unit	Whole System
$E_{in}$	kJ/kg-cl	533.98	1865.83	5498.71	1662.59	484.16	3187.29
Total effective heat	kJ/kg-cl	152.71	1266.03	1761.76	1577.07	79.60	2041.59
$\varphi^i$	%	28.60	67.85	32.04	94.86	16.44	64.05

**Figure 7.** Influence of subunits' thermal efficiency on  $\varphi^{QY}$ .

Calculations show that  $\varphi^{DC}$  carries the most influence on  $\varphi^{QY}$ , where every 1% increase in  $\varphi^{DC}$  leads to a 1.73% increase in  $\varphi^{QY}$ . Next are the Preheating and Cooling units, which have similar effects on  $\varphi^{QY}$  where a 1% increase in  $\varphi^P$  and  $\varphi^C$  increases  $\varphi^{QY}$  by 0.59% and 0.52%, respectively;  $\varphi^{RS}$  and  $\varphi^{CA}$  have the smallest impacts on  $\varphi^{QY}$ , as a 1% increase in  $\varphi^P$  and  $\varphi^{CA}$  only led to increases of 0.17% and 0.15% in  $\varphi^{QY}$ , respectively. Such results are consistent with most efforts and achievements of cement practitioners. One may conclude that efforts to improve efficiency should focus on the Decomposition and Clinker Calcination unit (D&C unit).

## 5. Application of the Thermal Efficiency Model

Application of the thermal efficiency model was carried out on a 5000 MT/D production line, which has the same process flow as the representative 5000 MT/D line in Section 4 and is denoted as "production line A". The rotary kiln of this line was  $\varphi$  4.8 m  $\times$  72 m, and the firing system uses a five-stage double series preheating system with a dual spout furnace. Its clinker output is 5799 MT/D with heat consumption of clinker at 3286.98 kJ/kg-cl.

### 5.1. Calculation of Thermal Efficiency before Optimization

Thermal calibration of the production line was carried out when the system was stable, and its main parameters are shown in Table 4 (data before optimization are also included in the table).

**Table 4.** Main parameters of the production line.

Parameters	Unit	Value	
		Before Optimization	After Optimization
Kiln coal	kg/kg.cl	0.0651	0.0518
Calcliner coal	kg/kg.cl	0.0714	0.0832
Secondary air	°C	1100	1109
	Nm <sup>3</sup> /kg.cl	0.423	0.293
Tertiary air	°C	902	912
	Nm <sup>3</sup> /kg.cl	0.455	0.549
Flue gas discharged from Preheating unit	°C	323.6	313.8
	Nm <sup>3</sup> /kg.cl	1.455	1.413
Dust discharged from Preheating unit	°C	323.6	313.8
	g/Nm <sup>3</sup>	80.32	84.59
Flue gas discharged from D&C unit	°C	860	860
	Nm <sup>3</sup> /kg.cl	1.457	1.416
Cooled clinker	°C	125	123
Decomposition rate of preheated meal into kiln	%	90	95
Flue gas discharged from rotary kiln	°C	1270	1150
	Nm <sup>3</sup> /kg.cl	0.563	0.549
Flue gas into AQC boiler	°C	339	369
	Nm <sup>3</sup> /kg.cl	0.860	0.860
Flue gas into coal mill	°C	250	250
	Nm <sup>3</sup> /kg.cl	0.114	0.114
Flue gas discharged from PH boiler	°C	220	220
	Nm <sup>3</sup> /kg.cl	1.457	1.416
Flue gas discharged from raw mill	°C	115	110
	Nm <sup>3</sup> /kg.cl	1.656	1.607

Thermal efficiency of the whole system before parameter optimization is calculated according to a thermal efficiency model; the results are shown in Table 5.

**Table 5.** Thermal efficiency of one 5000 MT/D production line before optimization.

Item	Units	R&S Unit	Preheating Unit	D&C Unit	Cooling Unit	C&A Unit	Whole System
$E_{in}$	kJ/kg-cl	684.97	2153.69	5852.42	1700.53	399.63	3286.98
Total effective heat	kJ/kg-cl	157.11	1391.52	1757.21	1620.97	66.45	2028.19
$\varphi^i$	%	22.94	64.61	30.03	95.32	16.63	61.70

## 5.2. Comparative Analysis of Thermal Efficiency and Optimization Suggestions

A comparison of the thermal efficiency of the whole system and subunits between production line A and the representative line is shown in Figure 8.

The thermal efficiencies of the subunits of production line A are lower than the values of the representative line, except for  $\varphi^{CA}$ ; as a result, the  $\varphi^{QY}$  of the production line A is only 61.70%, which is 2.35% lower than the representative line.

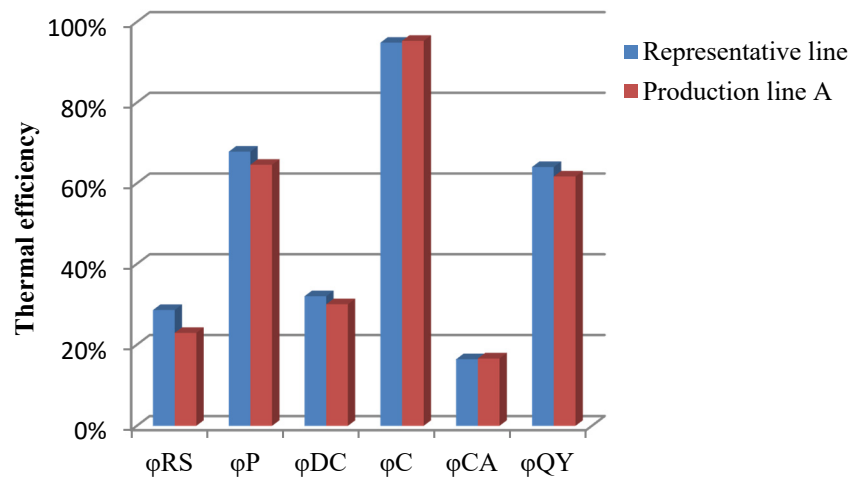


Figure 8. Comparison of thermal efficiency.

According to the thermal efficiency model, the main reason for the low thermal efficiency of the whole system is the low thermal efficiencies of the D&C and Preheating units. The reasons for these low  $\varphi^{DC}$  and  $\varphi^P$  were analyzed according to the parameters of the production line A (as shown in Table 4) as follows.

- (1) Low decomposition rate of preheated meal into the rotary kiln.

The decomposition rate of the preheated meal (raw feed) entering the rotary kiln in production line A is only 90%, which is lower than the recommended rate (no less than 95%). A portion of the calcium carbonate enters the kiln with preheated meal to be decomposed, absorbs heat in the rotary kiln and thus increases the thermal load of the kiln and restricts the clinker output increase. Consequently, surface heat loss per kilogram of clinker in the D&C system will be increased as the total heat dissipation per hour is constant.

- (2) Excess secondary air volume.

The oxygen content in the flue gas at the kiln hood is around 4.0%, which is higher than the recommended value of about 2%. This is an equivalent of an excess air coefficient of 1.18, which means that the volume of secondary air in the kiln is higher than its actual requirement. Excessive volume of secondary air results in increased sensible heat taken away by the flue gas discharged from the D&C unit.

- (3) Low heat transfer efficiency between gas and solid.

Heat transfer efficiency between the fed meal and flue gas in the Preheating system is mainly determined by the structural parameters and gas-solid ratio of the Preheating system. Heat transfer efficiency between gas and solid increases as the solid-gas ratio increases when structural parameters remain unchanged [24]. Affected by the excess secondary air, the solid-gas ratio of the preheating system at production line A is only 1.21, and the effect of heat transfer between the gas and solid is poor where the temperature of the exhaust gas from the preheating system unit is as high as 323.6 °C. Therefore, a large amount of heat is taken away with the flue gas, resulting in low thermal efficiency of the Preheating unit.

Based on the premise of maintaining the existing process route and main equipment, measures such as properly increasing the calcination temperature in the calciner or increasing the proportion of calciner coal and tertiary air can be taken to improve the decomposition rate of preheated meal in the kiln. At the same time, excess air coefficient of secondary air should be properly reduced to

reduce the sensible heat taken away by the high temperature flue gas discharged from the D&C unit. Furthermore, with decreased excess air coefficients, the solid-gas ratio of the Preheating unit can be slightly increased to improve the heat transfer between the gas and solid and thus,  $\varphi^P$  would be increased. Since both  $\varphi^{DC}$  and  $\varphi^P$  would increase, the thermal efficiency of the whole kiln system of production line A can be improved.

### 5.3. Calculation of Thermal Efficiency After Optimization

The main parameters of production line A after optimization are shown in Table 4 (parameters after optimization) and the thermal efficiency is also calculated as shown in Table 6.

**Table 6.** Thermal efficiency of one 5000 MT/D production line after optimization.

Item	Units	R&S Unit	Preheating Unit	D&C Unit	Cooling Unit	C&A Unit	Whole System
$E_{in}$	kJ/kg-cl	642.51	2090.87	5727.65	1662.86	435.83	3252.41
Total effective heat	kJ/kg-cl	152.46	1373.50	1757.74	1585.01	79.10	2036.73
$\varphi^i$	%	23.73	65.69	30.69	95.32	18.15	62.62

As seen in Tables 5 and 6, the  $\varphi^{QY}$  of production line A increased from 61.70% to 62.62% after parameter optimization. Measurements also confirmed that its clinker output increased from 5799 MT/D to 5968 MT/D, whereas the heat consumption of clinker was reduced from 3286.98 kJ/kg-cl to 3252.41 kJ/kg-cl; all of which shows that the thermal efficiency model plays a positive role in improving the thermal efficiency of the cement production line.

### 5.4. Summary of Thermal Efficiency Application

The thermal efficiency of one 5000 MT/D production line was analyzed using the whole system thermal efficiency model. The model found out that the main reason for the low thermal efficiency  $\varphi^{QY}$  lies in its low  $\varphi^{DC}$  and  $\varphi^P$ .  $\varphi^{DC}$  was improved by increasing the decomposition of preheated meal into the kiln, while  $\varphi^P$  was increased by reducing the excess air coefficient of secondary air as diagnosed by the model. The values of  $\varphi^{DC}$  and  $\varphi^P$  in the production line increased from 30.03% and 64.61% to 30.69% and 65.69%, respectively; as a result,  $\varphi^{QY}$  increased from 61.70% to 62.55%, and the clinker output and heat consumption of clinker were slightly optimized.

## 6. Conclusions

A thermal efficiency model of the whole clinker calcination system was established by mass/heat balance analysis of its subunits, and its application was carried out on one 5000 MT/D production line in this paper. The following conclusions were obtained:

1. The thermal efficiency of the whole system ( $\varphi^{QY}$ ) is linearly correlated with the thermal efficiencies of its subunits. Increases in the thermal efficiency of each subunit lead to increases in  $\varphi^{QY}$ .
2. The thermal efficiency of the D&C subunit,  $\varphi^{DC}$ , provided more influence than other subunits on the whole system. It was found that a 1% increase in  $\varphi^{DC}$  led to a 1.73% increase in  $\varphi^{QY}$ , followed by the Preheating unit and Cooling unit, where a 1% increase in  $\varphi^P$  and  $\varphi^C$  led to increases in  $\varphi^{QY}$  of 0.59% and 0.52%, respectively;  $\varphi^{RS}$  and  $\varphi^{CA}$  had the lightest impact on  $\varphi^{QY}$  where 1% increases in  $\varphi^P$  and  $\varphi^{CA}$  might only lead to increases of 0.17% and 0.15% in  $\varphi^{QY}$ , respectively.
3. Thermal efficiency of the whole system ( $\varphi^{QY}$ ) of one 5000 MT/D production line was 61.70% as calculated, which was 2.35% lower than the representative line. Application of the model revealed that this was due to low  $\varphi^{DC}$  and  $\varphi^P$  values derived from the low decomposition rates of calcium carbonate in the preheated meal in the kiln and the high excess air coefficient of secondary air.

4. After control parameter optimization based on the model,  $\varphi^{DC}$  and  $\varphi^P$  values of the production line increased from 30.03% and 64.61% to 30.69% and 65.69%, respectively, and as a result, the  $\varphi^{QY}$  increased from 61.70% to 62.55% and the clinker output and heat consumption of clinker were slightly optimized at the same time.

**Author Contributions:** Conceptualization, Y.C. and S.D.; methodology, Y.Y. and S.D.; data curation, Y.Y.; writing—original draft preparation, Y.Y.; writing—reviewing and editing, Y.C. and S.D.; scope and plot in draft, Y.Y.; writing—revising, S.D. All authors have read and agreed to the published version of the manuscript.

**Funding:** This research was funded by NATIONAL KEY R&D PROGRAM OF CHINA, grant number 2016YFB0303402.

**Conflicts of Interest:** The authors declare no conflict of interest.

## Nomenclature

Symbol	Content	Unit
$A_1$	Volume of flue gas at preheater outlet per kg clinker	$\text{Nm}^3$
$A_2$	Volume of exhaust gas at R&SP outlet per kg clinker	$\text{Nm}^3$
$C_1$	Specific heat of flue gas at preheater outlet	$\text{kJ}\cdot(\text{kg K})$
$C_2$	Specific heat of fly ash at preheater outlet	$\text{kJ}\cdot(\text{kg K})^{-1}$
$C_3$	Specific heat of exhaust gas at R&SP outlet	$\text{kJ}\cdot(\text{kg K})^{-1}$
$C_4$	Specific heat of raw materials at raw mill outlet	$\text{kJ}\cdot(\text{kg K})^{-1}$
$C_5$	Specific heat of water vapor at SP inlet	$\text{kJ}\cdot(\text{kg K})^{-1}$
$C_6$	Specific heat of water vapor at SP outlet	$\text{kJ}\cdot(\text{kg K})^{-1}$
$M_1$	Fly ash at preheater outlet per kg clinker	kg
$M_2$	Raw materials at raw mill outlet per kg clinker	kg
$M_3$	Water in raw materials at raw mill outlet per kg clinker	kg
$M_4$	Water vapor of SP boil per kg clinker	kg
$M_5$	Magnesium carbonate contained in raw materials to preheating unit per kg clinker	kg
$M_6$	Calcium carbonate contained in raw materials per kg clinker	kg
$T_0$	Ambient temperature	$^{\circ}\text{C}$
$T_1$	Temperature of flue gas at preheater outlet	$^{\circ}\text{C}$
$T_2$	Temperature of fly ash at preheater outlet	$^{\circ}\text{C}$
$T_3$	Temperature of exhaust gas at R&SP outlet	$^{\circ}\text{C}$
$T_4$	Temperature of raw materials at raw mill outlet	$^{\circ}\text{C}$
$T_5$	Temperature of R&SP surface	$^{\circ}\text{C}$
$T_6$	Temperature of water vapor at SP inlet	$^{\circ}\text{C}$
$T_7$	Temperature of water vapor at SP outlet	$^{\circ}\text{C}$
$\xi_1$	Heat transfer coefficient of R&SP surface	$\text{kJ}\cdot(\text{m}^2\cdot\text{K})^{-1}$
$S_1$	Superficial area of R&SP surface	$\text{m}^2$

## References

- Bildirici, M.E. Cement production, environmental pollution, and economic growth: Evidence from China and USA. *Clean Technol. Environ. Policy* **2019**, *21*, 783–793. [[CrossRef](#)]
- Wei, J.; Cen, K. Empirical assessing cement CO<sub>2</sub> emissions based on China's economic and social development during 2001–2030. *Sci. Total Environ.* **2019**, *653*, 200–211. [[CrossRef](#)] [[PubMed](#)]
- Andrew, R.M. Global CO<sub>2</sub> emissions from cement production, 1928–2017. *Earth Syst. Sci. Data* **2018**, *10*, 2213–2239. [[CrossRef](#)]
- Breidenbach, J. The new kiln line 6 at the Exshaw cement plant in Canada. *Cem. Int.* **2017**, *6*, 28–33.
- Ma, J.M.; Peng, X.P.; Di, D.R.; Zhao, L.; Chen, C.H.; Li, B.; Wang, W. Research and Application of the Cement Low-energy Consumption Burning Technology. *Cem. Technol.* **2019**, *3*, 21–28.
- Assawamartbunlue, K.; Surawattanawan, P.; Wanwiwa, L. Specific energy consumption of cement in Thailand. *Energy Procedia* **2019**, *156*, 212–216. [[CrossRef](#)]
- Wang, J.F.; Dai, Y.P.; Gao, L. Energy analyses and parametric optimizations for different cogeneration power plants in cement industry. *Appl. Energy* **2009**, *86*, 941–948. [[CrossRef](#)]

8. Rasul, M.G.; Widiyanto, W.; Mohanty, B. Assessment of the thermal performance and energy conservation opportunities in a cement industry in Indonesia. *Appl. Therm. Eng.* **2005**, *25*, 2950–2965. [[CrossRef](#)]
9. Su, T.L.; Chan, D.Y.L.; Hung, C.Y.; Hong, G.B. The status of energy conservation in Taiwan's cement industry. *Energy Policy* **2013**, *60*, 481–486. [[CrossRef](#)]
10. Nazari, M.A.; Aslani, A.; Ghasempour, R. Analysis of solar farm site selection based on TOPSIS Approach. *Int. J. Soc. Ecol. Sustain.* **2018**, *9*, 12–25. [[CrossRef](#)]
11. Zhou, C.Y.; Wang, Y.Q.; Jin, Q.Y.; Chen, Q.J.; Zhou, Y.G. Mechanism analysis on the pulverized coal combustion flame stability and NO<sub>x</sub> emission in a swirl burner with deep air staging. *J. Energy Inst.* **2019**, *92*, 298–310. [[CrossRef](#)]
12. Ma, L.; Fang, Q.Y.; Yin, C.G.; Wang, H.J.; Zhang, C.; Chen, G. A novel corner-fired boiler system of improved efficiency and coal flexibility and reduced NO<sub>x</sub> emissions. *Appl. Energy* **2019**, *238*, 453–465. [[CrossRef](#)]
13. Li, Q.; Xu, D.L.; Chen, Y.X.; Yao, Y.F.; Sun, Z.; Ding, S.X. Decomposition of ammonium sulfate residue in a high solid/gas ratio suspension state with an industrial-scale reactor system (production line). *Particuology* **2015**, *22*, 107–113. [[CrossRef](#)]
14. Du, Y.; Wu, X.L.; Tian, Q.; Meng, F.H.; Ren, H.P. Design and application of intelligence coordination control system for complicated industrial process. *J. Hebei Univ. Sci. Technol.* **2005**, *26*, 146–149.
15. Zhang, Y.L.; Wang, X.H.; Yu, H.L. Design of The Intelligent Control System of Cement Calciner. *J. Univ. Jinan Sci. Technol.* **2014**, *2*, 97–100.
16. Gang, X.; Fan, Y.; Keming, X. The Temperature Control of Cement Decomposing Furnace Based on Immune Neural Network. *J. Taiyuan Univ. Technol.* **2007**, *38*, 287–289.
17. Jarvensivu, M.; Saari, K.; Jounela, S.L.J. Intelligent Control System of an Industrial Lime Kiln Process. *Control. Eng. Pract.* **2001**, *9*, 589–606. [[CrossRef](#)]
18. Wang, X.H.; Fang, X.M.; Yu, H.L. Recognition of Working Condition for Rotary Kiln Hood Based on Expert System. *Control. Eng. China* **2010**, *5*, 309–312.
19. Chen, H.K.; Liu, H.Y.; Liu, D.P. Optimal Design of Rotary Kiln Control System Based on DCS. *J. Qilu Univ. Technol.* **2018**, *32*, 54–60.
20. Pramathes, D.; Chandrani, D. Distributed control system in cement industry. *J. Mines Metals Fuels* **2013**, *61*, 302–305.
21. Siwen, W.; Xiaodong, D.; Juju, H. Design of the control system of the new dry process cement production line. *J. Xinyu Coll.* **2009**, *14*, 94–96.
22. Tahsin, E.; Vedat, A. Energy auditing and recovery for dry type cement rotary kiln systems—a case study. *Energy Convers. Manag.* **2005**, *46*, 551–562.
23. Liu, Z.; Wang, Z. Thermal efficiency modeling of the cement clinker manufacturing process. *J. Energy Inst.* **2015**, *88*, 76–86. [[CrossRef](#)]
24. Delong, X. *Theory and Practice of Cement Suspension Pre-Decomposition Technology*; Scientific & Technical Documents Publishing House: Beijing, China, 2002; ISBN 7-5023-4272-9.



© 2020 by the authors. Licensee MDPI, Basel, Switzerland. This article is an open access article distributed under the terms and conditions of the Creative Commons Attribution (CC BY) license (<http://creativecommons.org/licenses/by/4.0/>).